Inorganica Chimica Acta 368 (2011) 21–28

Contents lists available at ScienceDirect

Inorganica Chimica Acta

journal homepage: www.elsevier.com/locate/ica

Zinc complexes with 1,2,4-triazole functionalized amino acid derivatives: Synthesis, structure and β-lactamase assay

Anil D. Naik [a], Joséphine Beck [a], Marinela M. Dîrtu [a], Carine Bebrone [b], Bernard Tinant [a], Koen Robeyns [a], Jacqueline Marchand-Brynaert [a], Yann Garcia [a,*]

[a] Institute of Condensed Matter and Nanosciences, Université Catholique de Louvain, Place L. Pasteur 1, 1348 Louvain-la-Neuve, Belgium
[b] Centre d'Ingénierie des Protéines, Université de Liège, B6-Sart Tilman, 4000 Liège, Belgium

ARTICLE INFO

Article history:
Received 19 August 2010
Received in revised form 1 December 2010
Accepted 9 December 2010
Available online 23 December 2010

Keywords:
1,2,4-Triazole
Zinc complexes
Amino acids
Trinuclear complex
β-Lactamase

ABSTRACT

Coordinating abilities of 4R-1,2,4-triazole derivatives (R = glycine ethyl ester (**L1**), glycine (**L2**), diethyl-amino malonate (**L3**), methionine (**L4**) and diethyl aminomethylphosphonate (**L5**)) towards Zn^{II} ions have been studied in solution, in solid state and versus three zinc-β-lactamases. The crystal structure of $[Zn_3(L4)_6(H_2O)_6]$ (**6**) is described; it is the first crystal structure involving a 1,2,4-triazole functionalized methionine. It forms a trinuclear complex with central zinc octahedrally coordinated by only **L4**, whereas terminal zinc ions coordination sphere is completed by three water molecules. **L4** exhibits a dual functionality of a bridging bidentate ligand as well as an anion. A dense hydrogen bonding network connects these trinuclear entity into a 3D supramolecular network. The Zn^{II} ions in **6** are held at equidistance (3.848 Å) which coincidently matches with the corresponding Zn···Zn distance in the binuclear zinc enzyme from *Bacillus cereus* (3.848 and 4.365 Å). Among **L1**–**L5** screened for β-lactamase assay, **L4** shows modest inhibition for *BcII* enzyme.

1. Introduction

Amino acids are the building blocks of proteins and the central trunk from which many diverse applied fields have branched out [1]. Not only amino-acids but also their derivatives have surfaced into biochemistry, pharmacology, peptide station, bio-mimics, enantioselective catalysis and separation, non-linear optics and materials science [1–3]. Advantage of these molecules is their natural miscellaneous framework with rich functional groups, which is amenable to copious derivatization. The diverse topology they adopt steering the crystal packing in molecular architectures through extended supramolecular interactions is intriguing [4–8]. Structure and reactivity of different amino acids in their natural or derivatized form were extensively studied; some elegant examples include proline [7a], glycine [7a], alanine [7b], aspartic acid [7c], phenyl alanine [7d], histidine [7e], methionine [7f–i] and typtophan [7j]. Diverse applications are quoted such as metal-peptide frameworks constructed from an oligovaline family [8a], a chiral metal Cu(II) cluster from dipeptidic *N*,*N*′-terephthaloyl-bis(*S*-aminocarboxylato) ligand [8b], a 2D Cu(II) network built from L-tryptophanato ligand [8c], coordination polymers of *N*-benzesulfonyl-L-glutamic acid [8d], and a chiral metal organic framework (MOF) from condensation product of glutamate moieties with xylene [4].

We recently introduced a simplified transamination reaction for converting the amine functional group of glycine into a 1,2,4-triazole [9]. Our interest in amino acid derivatization was fuelled by promising results shown by 1,2,4-triazole-carboxylate derivatives in synthetic chemistry [9], spin crossover phenomenon [10] and nanoporous MOFs [11]. Applications envisioned in these fields largely depend on molecular conformations these precursors adopt during the self-assembly process which directs structure-properties relationships. Here we introduce a set of natural and non-natural amino acids selected for their functional group diversity to functionalize into 1,2,4-triazoles (Scheme 1). Such groups (*N*-heterocycle, acid, carboxylate, phosphate and thiomethyl) could be potential ligands of M^{II} cations, in particular Zn^{II} is found as co-factor in several metallo-proteases.

Thus in continuation of our transamination strategy [9], exemplified with ligands **L1** and **L2**, we introduce new tailored 4R-1,2,4-triazoles from amino-acid and amino-acid esters, namely diethyl aminomalonate (**L3**), methionine (**L4**) and diethyl aminomethylphosphonate (**L5**) (Scheme 1). Their coordinating abilities towards Zn^{II} along with ligands from glycine ethyl ester (**L1**) and glycine (**L2**) [9] have been studied in solution, in solid state and versus three zinc-β-lactamases.

* Corresponding author. Fax: +32 10 472330.
E-mail address: yann.garcia@uclouvain.be (Y. Garcia).

0020-1693/$ - see front matter © 2010 Elsevier B.V. All rights reserved.
doi:10.1016/j.ica.2010.12.017

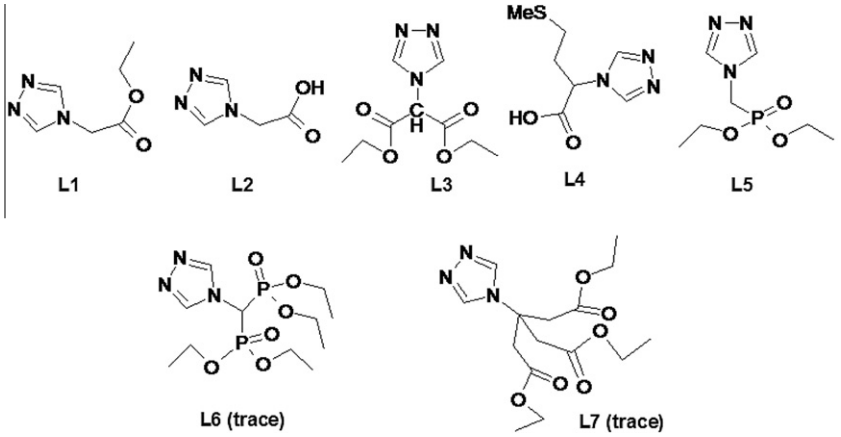

Scheme 1. 4-R-1,2,4-Triazoles derived from aminoacids.

2. Experimental

2.1. Chemicals

All reagents and solvents were used as received from commercial sources: benzene, *N*,*N*-dimethylformamide, (Sigma–Aldrich), glycine ethyl ester hydrochloride, diethyl aminomalonate hydrochloride, *p*-toluene sulfonic acid, thionyl chloride, (Acros), DL-methionine (Janssen chimica), aq. hydrazine hydrate (Aldrich), $Zn(OAc)_2{\cdot}2H_2O$ (UCB), and $ZnCl_2$ (Fluka).

2.2. Instrumentation

^1H and ^{13}C NMR spectra were recorded at 300 MHz and 75 MHz, respectively, on a Bruker AC300 instrument. The residual solvent peak was used as internal reference. FTIR spectra were recorded on a Bio-Rad FTS 135 spectrometer using KBr discs. Mass spectral data were obtained on Thermo Finnigan LCQ Ion trap spectrometer (APCI mode). HRMS were carried out on a Micromass Q TOF 2 spectrometer in ESI mode, detecting positive ions. CHN analyses were performed at the University College London (UK). TGA-DTA analyses were performed in air at a heating rate of 10 K/min (298–1173 K) using an Universal V2.5H TA instrument. Zn% was determined from ZnO residue obtained from TGA analysis of all freshly prepared zinc complexes that were preliminary dried in air. Powder X-ray diffraction patterns were recorded on a Siemens D5000 counter diffractometer working with a Kα radiation (1.5418 Å) at 293 K. Melting points were determined with an oil bath 3937-S Buchi device. Column chromatography was performed on silica gel 60 (63–200 mesh, Merck). Scanning electron microscopy (SEM) coupled with EDX was performed with a Gemini Digital Scanning Microscope 982 with 1 kV accelerating voltage using an aluminium sample holder. Solid state emission spectra were recorded on Fluorolog-3 (Jobin-Yvon-Spex) spectrometer. Activity test were monitored by using an UvikonXL spectrophotometer connected to a computer via a RS232 serial interface. Diffuse reflectance spectra were recorded with a CARY 5E spectrophotometer using Teflon as a reference.

2.3. β-Lactamase assay

L1–**L5** were screened for inhibition against three representative metallo-β-lactamases, namely *BcII* from *Bacillus cereus* [12], *CphA* from *Aeromonas hydrophila* [13] and *L1* from *Stenotrophomoncas maltophilia* [14] representing B1, B2 and B3 sub-classes. **L1**, **L2**, **L3**, and **L5** were prepared as 10 mM in water solutions and **L4** as 10 mM in DMSO solution before dilution with appropriate buffers. Buffers were, respectively, 10 mM Hepes pH 7.5 for BcII, 15 mM Cacodylate pH 6.5 for CphA and 20 mM Hepes pH 7.0 for *L1*. The three buffers were prepared with Milli-Q water and Zn^{II} residual concentration was below 0.4 μM. Tests verified that the low concentration of DMSO present had no inhibition effect: the rate remained the same upon addition of 1% DMSO. *BcII*, *CphA*, and *L1* enzymes were used at concentrations of 8, 1.6 and 1.4 nM, respectively. The enzyme and the 100 μM inhibitor were pre-incubated 30 min in a volume of 490 mL at room temperature. Then, 10 μL of 5 mM imipenem were added and the hydrolysis of imipenem was monitored by following the variation in absorbance at 300 nm, using an UvikonXL spectrophotometer connected to a computer via a RS232 serial interface. The experiments were performed at 30 °C and initial rate conditions were used to study the inhibition with imipenem. The assays were made in triplicate; the error was less than 5%.

3. Synthesis

3.1. Synthesis of ligands

N,*N*-dimethylformamide azine dihydrochloride (**a**) and its free base (**b**) are obtained following Refs. [15,16] (Scheme 2); **b** was recrystallised from benzene with charcoal as colourless flakes and used in following transamination reactions (*Caution:* all operations concerned with benzene, which is a possible carcinogen, should be carried out in an efficient fume hood). Diethyl aminomethylphosphonate was prepared by the reported methods [17,18]. Synthesis of ethyl 4H-1,2,4-triazol-4-yl-acetate (**L1**), 4H-1,2,4-triazol-4-yl acetic acid (**L2**) were carried out following [9].

3.1.1. Diethyl 4H-1,2,4-triazol-4-yl malonate (*L3*)

The reaction was carried out in a dry round-bottomed flask fitted with a reflux condenser. Solid **b** (500 mg, 3.5 mmol) was added under stirring to a suspension of diethyl aminomalonate hydrochloride (745 mg, 3.5 mmol) in benzene (30 mL) at approximately 60 °C. The mixture was refluxed for 24 h with vigorous stirring. The reaction can be monitored by running thin layer chromatography at interval of time. Finally, solvent was removed under vacuum and chromatographic purification (SiO_2, $CH_2Cl_2 \rightarrow$ 5% isopropanol in CH_2Cl_2) afforded a yellow oil, which upon repeated crystallization from ether-methanol mixture provided a white hygroscopic solid (0.45 g, 56%), m.p 63 °C. R_f 0.3 (5% isopropanol in CH_2Cl_2). FTIR (KBr, cm^{-1}): 3126(w), 1743(vs), 1523(m), 1303(vs), 1193(vs), 1020(vs), 869(s). ^1H NMR

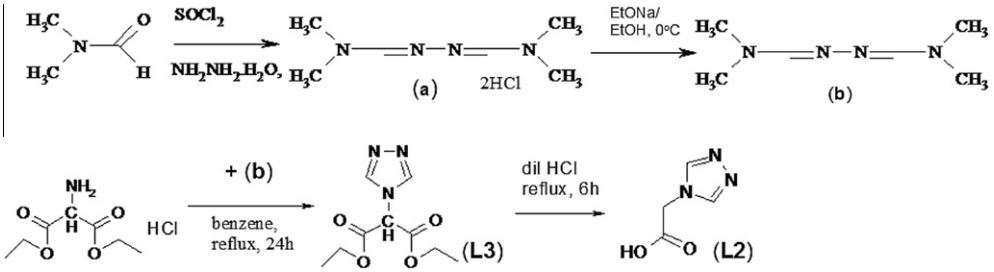

Scheme 2. Synthetic protocol used for **L3**.

(300 MHz, $CDCl_3$, 298 K): δ = 8.6 (s, 2H), 5.86 (s, 1H), 4.28–4.36 (m, 4H), 1.31 (t, 6H). ^{13}C NMR (75 MHz, $CDCl_3$, 298 K): δ = 163.5, 142.8, 63.9, 60.77,14.01, MS: m/z = 228.14 ($M+H^+$). *Anal.* Calc. for $C_9H_{13}N_3O_4{\cdot}H_2O$ (245.10): C, 44.06; H, 6.17; N, 17.14. Found: C, 44.56; H, 5.75; N, 17.21%. Refluxing **L3** with 6 N HCl leads to hydrolysis followed by decarboxylation. Analysis on the product confirms formation of **L2** (Lit. [9], m.p 161 °C).

*3.1.2. 4-(methylthio)-2-(4H-1,2,4-triazol-4-yl)Butanoic acid (**L4**)*

DL-methionine (100 mg, 0.67 mmol) was suspended in benzene (20 mL) and warmed to 70 °C. Solid azine dihydrochloride **a** (144 mg, 0.67 mmol) was added with stirring and the mixture further refluxed for 24 h with vigorous stirring. A pale yellow viscous mass was obtained. Solvent was evaporated under reduced pressure and the residue dissolved in dry MeOH (4 mL). Insoluble residue was filtered off, and solvent evaporated to yield a pale yellow viscous solid. The residue was redissolved in $CHCl_3$ (20 mL), dried over sodium sulfate and filtered. The filtrate was cooled in refrigerator overnight. Colourless needles obtained were filtered, dried and stored in desiccator. m.p 94 °C. Yield 0.1 g (75%). FTIR (KBr, cm^{-1}): 3417(br), 1712(s), 1635(s), 1467(m), 1188(m), 1022(s), 887(m). ^1H NMR (300 MHz, DMSO-d_6, 298 K): δ = 8.64 (s, 2H), 5.28 (*t*, 1H, J = 7.2 Hz), 2.27–2.40 (m, 4H), 2.06 (s, 3H). ^{13}C NMR (75 MHz, DMSO-d_6, 298 K): δ = 172.2, 145, 58.7, 32.8, 31.2, 15.3. APCI MS m/z = 202.04 (M+1). *Anal.* Calc. for $C_7H_{11}N_3O_2S$ (201.25): C, 41.78; H, 5.51; N, 20.88. Found: C, 41.68; H, 5.46; N, 21.48%.

*3.1.3. Diethyl 4H-1,2,4-triazol-4-yl methylphosphonate (**L5**)*

The same synthetic procedure used for **L3** (amine 50 mg, 0.29 mmol; 38.6 mg of **b**, 0.27 mmol) was followed but with a catalytic amount of *p*-toluene sulfonic acid. The yellow oil obtained after solvent evaporation was dissolved in CH_2Cl_2 and washed with a saturated NaCl solution that was basified with sodium carbonate (pH 8–9). The organic layer was dried over sodium sulfate, solvent removed under vacuum and the yellow oil thus obtained was dried under vacuum. FTIR (film, cm^{-1}): 2983(m), 1643(br, m), 1548(m), 1444(m), 1392(m), 1230(s), 1163(m), 1010(s), 970(s), 794(m), 605(s). ^1H NMR (300 MHz, $CDCl_3$, 298 K): δ = 8.23 (s, 2H), 4.32 (d, 2H, $J_{P,H}$ = 12.9 Hz), 4.05–4.15 (m, 4H), 1.27 (t, 6H). ^{13}C NMR (75 MHz, $CDCl_3$, 298 K): δ = 143.3, 63.68 (d, $J_{C,P}$ = 7 Hz), 41.18 (d, $J_{C,P}$ = 158 Hz), 16.5. APCI MS: m/z = 219.71 ($M+H^+$). HRMS calcd. for $C_7H_{15}N_3O_3P$: 220.0851. Found: 220.0847.

3.2. Synthesis of complexes

*3.2.1. $[Zn(L1)_2(OAc)_2]$ (**1**)*

A methanolic solution (2 mL) of $Zn(OAc)_2{\cdot}2H_2O$ (35.4 mg, 0.16 mmol) was added to a methanolic (2 mL) solution of **L1** (50 mg, 0.32 mmol). The mixture was stirred slowly at r.t. and the progress of the reaction monitored by ^1H NMR at an interval of 0.5 h for 2 h. After reaction completion, solvent evaporation gave a colourless oil (**1**). Yield 78 mg (100%) FTIR (cm^{-1}): 3126(w), 1748(s), 1595 (br, s), 1385(s), 1076(m), 1023(m), 677(s), 635(m). ^1H NMR (300 MHz, CD_3OD, 298 K): δ = 8.62 (s, 4H), 5.1 (s, 4H). 3.61 (*q*, 4H, J = 7.05 Hz), 1.18 (*t*, 6H, J = 7.05), 2.05 (s, 6H, CH_3 of acetate). ^{13}C NMR (75 MHz, CD_3OD, 298 K): δ = 181.2, 169.8, 147.3, 59.2, 48.07, 23.1, 19.2. ESI-MS: cluster of peaks at m/z = 493 corresponds to [M+H$^+$] (calc. 492.09).

*3.2.2. $[Zn(L1)_2Cl_2]{\cdot}3MeOH$ (**2**)*

Reaction of $ZnCl_2$ (22 mg, 0.16 mmol) in MeOH (5 mL) with **L1** (50 mg, 0.32 mmol) in MeOH (5 mL) resulted in the isolation of a white precipitate (**2**) which was dried in air. Yield 35 mg, (50%). FTIR (KBr, cm^{-1}): 3130(m), 1747(vs), 1556(m), 1247(s), 1224(s), 1029(m), 630(m). ^1H NMR (300 MHz, d_6-DMSO, 298 K): δ = 8.56 (s, 4H), 5.09 (s, 4H). 4.20 (*q*, 4H, J = 7.11 Hz), 1.25 (*t*, 6H, J = 7.11). ^{13}C NMR (75 MHz, d_6-DMSO 298 K): δ = 168, 144.8, 62.2, 46.26, 14.77. ESI-MS: cluster of peaks at m/z = 444.78, ([M+H$^+$] (calc. 444.0). The sample begins to loose solvent molecule over a period of time. *Anal.* Calc. for $C_{12}H_{18}N_6O_4ZnCl_2{\cdot}MeOH$: C, 32.77; H, 4.66; N, 17.65; Zn, 12.05. Found: C, 31.86; H, 3.61; N, 17.89; Zn, 11.5%. Degradation temperature by DTA (onset point): 240(1) °C.

*3.2.3. $[Zn(L2)_2]{\cdot}CH_3OH$ (**3**)*

$Zn(OAc)_2{\cdot}2H_2O$ (43.2 mg, 0.196 mmol) dissolved in MeOH (2 mL), was added with stirring to a methanolic (2 mL) solution of **L2** (50 mg, 0.39 mmol) at r.t. The mixture was stirred for 15 min and the white precipitate obtained was filtered, washed with MeOH (1 mL) and dried in air (**3**). Yield 51 mg (80%). FTIR (KBr, cm^{-1}): 3089(m), 1743(m), 1735(m), 1641(s), 1560(m), 1392(s), 1230(m), 1039(m), 919(w), 790(m), 698(m), 634(m). ^1H NMR (300 MHz, D_2O, 298 K): δ = 10.58 (s, 4H), 6.8 (s, 4H). ^{13}C NMR (75 MHz, D_2O, 298 K): δ = 175.5, 147.7, 51. *Anal.* Calc. for $C_8H_8N_6O_4Zn$ (315.98): C, 30.38; H, 2.55; N, 26.59; Zn, 18.37. Found: C, 29.88; H, 3.76; N, 26.13l Zn, 18.90%.

*3.2.4. $[Zn(L3)_2(Cl)_2]$ (**4**)*

L3 (50 mg, 0.22 mmol) was dissolved in MeOH (2 mL) and to this was added $ZnCl_2$ (15 mg, 0.11 mmol) in MeOH (2 mL). Reaction was completed within 30 min and concentration of reaction mixture yielded a yellow oil (**4**). Yield 65 mg, (100%). FTIR (film, cm^{-1}): 1742(br, s), 1698(s), 1544(m), 1371(m), 1307(s), 1020(s), 891(m), 639(s). ^1H NMR (300 MHz, $CDCl_3$, 298 K): δ = 8.81 (s, 2H), 6.1(s, 1H), 4.21–4.28 (q, 4H), 1.33 (*t*, 6H, J = 7.11 Hz). ^{13}C (75 MHz, $CDCl_3$, 298 K): δ = 163.4, 144.9, 64.2, 61.4, 14.0. ESI MS shows packet of peaks centred around 552 corresponding to [Zn + 2L3 + Cl]$^+$. Peak found at 781 was calculated as [Zn + 3L3 + Cl]$^+$.

*3.2.5. $[Zn_3(L4)_6(MeOH)_6]$ (**5**) and $[Zn_3(L4)_6(H_2O)_6]$ (**6**)*

$Zn(OAc)_2{\cdot}2H_2O$ (54 mg, 0.49 mmol) in MeOH (2 mL) was added with stirring to a methanolic solution of **L4** (100 mg, 0.98 mmol) at r.t. resulting immediately in a pale yellow precipitate. The mixture was stirred for 15 min, filtered, washed with MeOH (1 mL) and dried in air to afford a white precipitate (**5**). Yield 150 mg (65%).

FTIR (KBr, cm^{-1}): 3485(br), 1647(s), 1382(m), 1197(m), 1078(m), 885(m), 667(m). ^1H NMR (300 MHz, DMSO-d_6, 298 K): δ = 8.67 (s, 4H), 5.01–5.05 (m, 2H), 2.32–2.41 (m, 8H), 2.05 (s, 6H). ^{13}C NMR (75 MHz, DMSO-d_6, 298 K): δ = 173.3, 144.5, 59.4, 33, 30.6, 15.4. Diffuse reflectance spectra (λ_{max}, nm), 270, 325 nm. *Anal.* Calc. for $C_{48}H_{84}N_{18}O_{18}S_6Zn_3$: C, 36.36; H, 5.34; N, 15.91; Zn, 12.11. Found: C, 36.48; H, 4.92; N, 15.52; Zn, 12.60%. **5** was recrystallized in H_2O/MeOH (3:1) affording colourless blocks, after slow evaporation for about two weeks, of formula $[Zn_3(L4)_6(H_2O)_6]$ (**6**) whose structure was determined by X-ray crystallography.

3.2.6. $[Zn(L5)_2(OAc)_2]$ (**7**)

A qualitative test has been made to check the coordinating ability of **L5** to zinc. The reaction mixture of **L5** (25 mg, 0.11 mmol) and $Zn(OAc)_2{\cdot}2H_2O$ (12.47 mg, 0.057 mmol) salt was stirred in $CDCl_3$ at r.t. for 20 min. before recording ^1H NMR. All signals undergo downfield shift relative to ligand (δ = 8.80(s), 4.62(d), 4.4–4.5(m), 1.32(t) and acetate at 1.95) along with some breakdown products. The shift is higher for triazole proton which is most likely coordinated to zinc. Continuation of reaction leads to appearance of more breakdown products as seen in NMR. The composition was concluded based on a mass spectral peak around 562 which corresponds to [M-OAc].

4. Single crystal X-ray diffraction

X-ray diffraction data were collected at 120 K for **6** with a MAR345 image plate using Mo Kα (λ = 0.71069 Å) radiation. The crystal was chosen, transferred to inert oil and mounted to the cold N_2-gas stream for flash cooling. The unit cell parameters were refined using all the collected spots after the integration process. The data were not corrected for absorption, but the data collection mode partially takes the absorption phenomena into account. The structure was solved by direct methods and refined by full-matrix least-squares on F^2 using SHELXL97 [19]. Non-hydrogen atoms were refined with anisotropic temperature factors. Hydrogen atoms were placed at calculated positions refined in the riding mode with isotropic temperature factors fixed 1.2 times $U_{(eq)}$ of the parent atoms (1.5 times for the methyl group).

5. Results and discussion

5.1. Synthesis and characterization

Amine derivatization into heterocycles, particularly tetrazole and 1,2,4-triazole, is greatly sought in coordination chemistry due to their diverse applications [20–22]. Whereas the Bayer method [23] was routinely employed for 1,2,4-triazole synthesis, 'transamination' was proved to be an advantageous synthetic strategy to derivatize mainly primary amine into a 1,2,4-triazole [15]. Amine exchange process with glycine was successfully carried out in a single step reaction without chromatographic purification [9]. Moderate yield led us to revisit the synthesis and to employ an ester of glycine precursor affording **L1** which can be easily hydrolysed to 4H-1,2,4-triazol-4-yl acetic acid (**L2**). This procedure not only improved the overall synthetic method but also introduced a versatile precursor in coordination chemistry [10,11]. Scheme 1 gives an overview of the transformed amino acids via the transamination process. **L1**, **L3** and **L5** were prepared using the standard protocol. **L2** could be obtained by hydrolysis of **L3** (Scheme 2) and **L4** was obtained without any catalyst [9]. Two bulky amines, namely tetraethyl aminomethyldiphosphonate [24,25] and triethyl aminocitrate [26,27] only provided a limited amount of triazoles **L6** and **L7,** which may be due to steric factors associated with the reactants. Indeed, the amino acid precursors did not react neither with **a** nor **b** under experimental conditions of variation of solvents and catalyst (benzene/toluene; with/without catalyst). All these hygroscopic molecules (**L1**–**L5**) are soluble in water, MeOH, DMF and DMSO.

Coordinating affinities of these ligands towards Zn^{II} were first studied in solution. Complexes were synthesized either with $ZnCl_2$ or $Zn(OAc)_2$ in MeOH at r.t. and the reaction was followed by ^1H NMR. Complexes formed with **L1**, **L3** and **L5** were quite sensitive to solvent medium, temperature, duration of reaction and work-up because of potential hydrolysis except for a few as explained below.

$[Zn(L1)_2(anion)_2]{\cdot}Solv$ complexes were obtained as a colourless oil (**1**, anion = OAc, Solv = 0) or a white precipitate (**2**, anion = Cl, Solv = 3 MeOH). Their formula was derived after characterization by NMR, IR, MS, CHN and TGA analyses. Zinc coordination exclusively occurs through nitrogen atoms of the triazole unit because the ester functionality is not affected, as concluded by IR and NMR spectroscopies. Prolonged stirring of reaction mixture of **1**–**2** leads to isolation of white precipitate which from NMR and IR studies was found to be a Zn^{II} complex including an hydrolyzed ligand (**L2**). Complex **3** was obtained as white powder. Here unlike **1** and **2**, the coordination competition between the triazole and the carboxyl group is in favour of the latter group through deprotonation as concluded by NMR. The strong absorption of carboxylic group around 1735 cm^{-1} in **L2** was not only shifted to 1743 cm^{-1} but appeared with reduced intensity as seen by IR spectroscopy further supports this formula $[Zn(L2)_2]{\cdot}CH_3OH$. A TGA analysis also supported the presence of a non-coordinated methanol molecule.

$[Zn(L3)_2Cl_2]$ (**4**) was obtained as a yellow oil and characterized by mass spectrometry. Reaction of $Zn(OAc)_2{\cdot}2H_2O$ with two equiv. of **L3** afforded too a yellow oil. However, the susceptibility of the ester functionality towards decarboxylation/hydrolysis was evident from ESI-MS as only a noticeable peak at m/z = 392 was found, corresponding to [Zn(L2)(OAc)], a breakdown product. Continuation of the reaction leads to complete hydrolysis and decarboxylation within 1 h giving a white precipitate which was analysed as **3**.

$[Zn_3(L_4)_6(MeOH)_6]$ (**5**) could be obtained as a white crystalline precipitate after having reacted $Zn(OAc)_2{\cdot}2H_2O$ with two equiv of **L4**. Absence of acetate anion was confirmed by NMR and IR spectroscopy. Carboxylic stretching in **L4** found at 1712 cm^{-1} in the IR spectrum, is no longer observed in **5**. Instead, a broad band around 1647 cm^{-1} is detected which could be either due to coordination to zinc or involvement in H-bonding interactions (Fig. S1). Crystal structure determination (*vide infra*) cleared this ambiguity as the carboxylic group was found to be not involved in coordination and actually present in a deprotonated form.

SEM images (Fig. 1) reveal the morphology of microcrystals (~400 nm thickness and ~1.74 μm width) in **5**. Most of crystals appear bent probably due to high vacuum conditions in the SEM instrument where solvent loss is expected. TGA (Fig. S1) of air dried sample shows in a first step, loss of three molecules of MeOH and further, the desolvated complex decomposes in two steps. **L4** shows fluorescence emission around 450 nm which is blue shifted to 425 nm in **5** with increased intensity. Such emission band in **5** is assigned to intraligand charge transfer (Fig. 1). The enhancement of fluorescence may be attributed to ligand chelation to metal centre which effectively increases the rigidity of the polynuclear complex and reduces the loss of energy by vibrational motion [28]. Recrystallization of **5** in a water/methanol medium led to the trinuclear complex **6** where the terminal bound MeOH molecules were replaced by water molecules as shown below by X-ray diffraction. $[Zn(L5)_2(OAc)_2]$ (**7**) was obtained by reacting **L5** with $Zn(OAc)_2{\cdot}2H_2O$ in $CDCl_3$, and its formula determined by mass spectrometry.

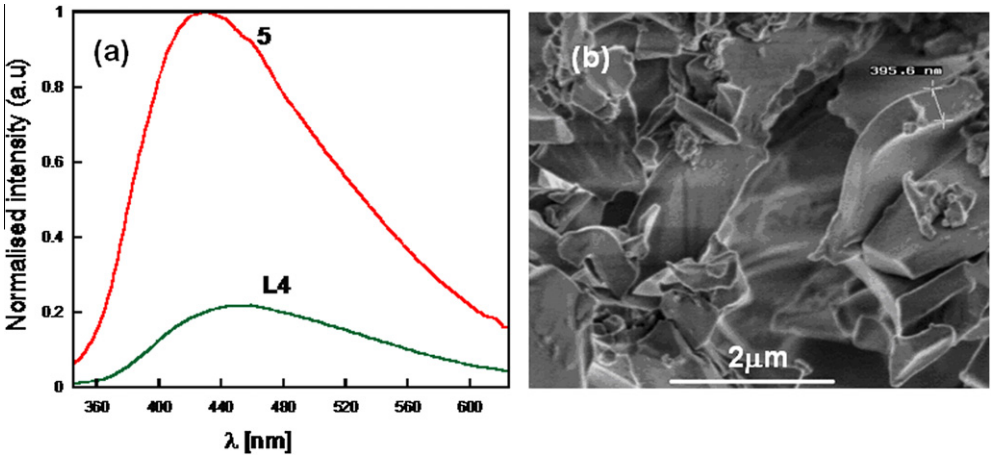

Fig. 1. (a) Solid state emission spectra of **L4** and **5**. (b) SEM on powder sample of **5**.

5.2. Crystal structure of *6*

$[Zn_3(L4)_6(H_2O)_6]$ (**6**) crystallizes in a trigonal space group (R-3c) at 120 K with Z = 36. Crystallographic information is gathered in Tables 1 and 2. It forms a trinuclear complex with three Zn^{II} ions in octahedral coordination (Fig. 2a) thanks to **L4** acting as a μ-*N1*,*N2*-bridging ligand. The three ligands bridging two Zn^{II} ions form a 'paddle wheel' motif with triazoles planes as propellers. The central Zn^{II} ion is surrounded by six nitrogen atoms belonging to six ligands with Zn1–N1 = 2.159(4) Å and forms a perfect octahedral geometry of ZnN_6 (N1–Zn1–N1, 180°(3)), while terminal Zn^{II} ions are coordinated by three nitrogen atoms (Zn2–N5, 2.145(4) Å) from three triazole ligands and three water molecules (Zn2–O14, 2.107(4) Å) forming a ZnN_3O_3 coordination sphere (with N5–Zn2–O14, 178.4(1)°). In case of a triple *N*1,*N*2-triazole bridge, the metal ions are located on the trigonal axis and any strain in the enclosed ring can be evaluated based on the N–M–N and N–N–M angles deviation to 90° and 125.26°, respectively [29]. In the present case, there is no strain in the ring as demonstrated by the angles N1–Zn1–N1 = 90.4(1)°, N5–Zn2–N5 = 90.1(1)° and N5–N1–Zn1 = 124.3(3)°, N1–N5–Zn2 = 125.8(3)°. The dihedral angle of N2–Zn2–Zn1–N1, which is a measure of the angle between any two of three triazole planes, is reaching 120° as expected (119.4(1)°).

Table 1
Crystallographic data and structure refinements for **6**.

Parameters	
Empirical formula	$C_7H_{14}N_3O_4S\ Zn_{0.5}$
T (K)	120(2)
M (g/mol)	268.96
Crystal system	trigonal
Space group	R-3c
a (Å)	15.249(5)
c (Å)	56.149(9)
V (Å^3)	11 307(6)
Z	36
ρ (g cm^{-3})	1.422
Crystal size (mm)	0.2 × 0.2 × 0.12
F(0 0 0)	5040
Reflections collected	36 600
Independent reflections	2311[$R_{(int)}$ = 0.062]
Goodness-of-fit (GOF) on F^2	1.063
R_1, wR_2 [$I > 2\sigma(I)$][a]	R_1 = 0.0832, wR_2 = 0.2727
R_1, wR_2 [all data]	R_1 = 0.0919, wR_2 = 0.2839
Largest difference in peak and hole (e Å^{-3})	1.418, and −0.717

[a] $R_1 = \sum||F_o| - |F_c||/\sum|F_o|$ for observed reflections, $wR_2 = [\sum wF_o^2 - F_c^2)^2/\sum wF_o^2]^{1/2}$, $w = 1/(\sigma^2(F_o^2) + 0.025F^2)$, $F = (2F_o + F_c)^3$.

A total of six **L4** ligands bridge in a bidentate fashion three Zn^{II} ions which are equidistant (Zn···Zn = 3.848 Å). This distance coincidently matches with that of a known binuclear Zn^{II} metalloenzyme from *B. cereus* (3.848 and 4.365 Å) [30] and is typical of trinuclear zinc complexes, e.g. $[Zn_3(etrz)_6(H_2O)_6](CF_3SO_3)_6$ [31] with Zn···Zn = 3.815(1) Å. Across the central Zn^{II}, on either side,

Table 2
Selected bond distances (Å), and bond angles (°) in **6**.

Bond lengths (Å)		Bond angles (°)	
Zn1–N1#1	2.159(4)	N1#1–Zn1–N1#2	90.40(15)
Zn1–N1#2	2.159(4)	N1#1–Zn1–N1#3	90.40(15)
Zn1–N1#3	2.159(4)	N1#2–Zn1–N1#3	90.40(15)
Zn1–N1#4	2.159(4)	N1#1–Zn1–N1	89.60(15)
Zn1–N1#5	2.159(4)	N1#2–Zn1–N1	180.0(3)
Zn1–N1	2.155(4)	N1#3–Zn1–N1	89.60(15)
Zn2–O14	2.107(4)	N1#1–Zn1–N1#4	180.0(3)
Zn2–O14#4	2.107(4)	N1#2–Zn1–N1#4	89.60(15)
Zn2–O14#5	2.107(4)	N1#3–Zn1–N1#4	89.60(15)
Zn2–N5#5	2.145(4)	N1–Zn1–N1#4	90.40(15)
Zn2–N2#4	2.145(4)	N1#1–Zn1–N1#5	89.60(15)
Zn2–N2	2.145(4)	N1#2–Zn1–N1#5	89.60(15)
N1–N5	1.375(6)	N1#3–Zn1–N1#5	180.0(4)
C7–O8	1.213(8)	N1–Zn1–N1#5	90.40(15)
C7–O9	1.223(8)	N1#4–Zn1–N1#5	90.40(15)
C11A–S12A	1.80(2)	O14–Zn2–O14 #5	92.25(15)
C13A–S12A	1.837(17)	O14–Zn2–O14#4	92.25(15)
C11B–S12B	1.81(3)	O14#5–Zn2–O14 #4	92.25(15)
S12B–C13B	1.81(2)	O14–Zn2–N5#5	178.43(15
		O14#5–Zn2–N5#5	88.56(15)
		O14#4–Zn2–N5#5	89.05(16)
		O14–Zn2–N5#4	89.05(16)
		O14#5–Zn2–N5#4	178.43(15)
		O14#4–Zn2–N5#4	88.56(15)
		N5#5–Zn2–N5 #4	90.12(15)
		O14–Zn2–N5	88.56(15)
		O14#5–Zn2–N5	89.05(16)
		O14#4–Zn2–N5	178.43(15)
		N5#5–Zn2–N5	90.12(15)
		N5#4–Zn2–N5	90.12(15)
		C2–N1–Zn1	128.5(3)
		N5–N1–Zn1	124.3(3)
		O8–C7–O9	125.8(6)
		C10–C11A–S12A	118.4(16)
		C11A–S12A–C13A	100.7(11)
		C10–C11B–S12B	126(3)
		C13B–S12B–C11B	108.7(17)
		Zn2–O14–H14A	114.1
		Zn2–O14–H14B	107.0

Symmetry transformations used to generate equivalent atoms: #1 $x-y, x-1, -z$; #2 $-x+2, -y, -z$; #3 $y+1, -x+y+1$; #4 $-x+y+2, -x+1, z$; #5 $-y+1, x-y-1, z$.

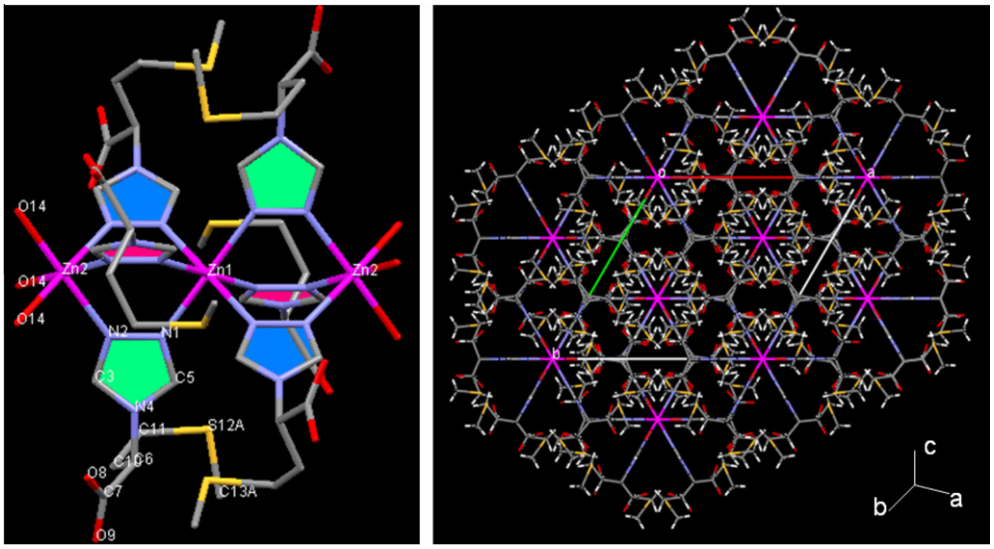

Fig. 2. (a) Molecular structure of **6**. (b) Crystal packing view of hexagonally arranged 'oval shaped' channels.

Table 3
H-bonding interactions in **6**.

D–H···A	*d*(D–H) (Å)	d(H···A) (Å)	*d*(D···A) (Å)	∠D–H···A (°)	Translation
O(14)–H(14A)···O(8)	0.86	1.85	2.697(7)	169	$1/3 + x - y, 2/3 - y, 1/6 - z$
O(14)-H(14B)···O(9)	0.86	2.01	2.656(11)	132	$7/3 - x, 2/3 - x + y, 1/6 - z$
O(15)-H(15A)···S(12A)	0.86	2.81	3.553(10)	146	$y, 1 - x + y, -z$
C(2)-H(2)···O(15)	0.95	2.60	3.520(11)	165	$1 + x - y, x, -z$
C(4)-H(4)···O(8)	0.95	2.53	3.384(7)	149	$1/3 + x - y, 2/3 - y, 1/6 - z$
C(6)-H(6)···S(12A)	1.00	2.83	3.193(9)	102	
C(13A)-H(13B)···O(9)	0.98	2.56	3.16(2)	120	$2 - x, 1 - y, -z$

the tripod of triazole planes adopt a 'staggered' arrangement due to steric requirements and interestingly three aqua ligands on each terminal zinc too adopt same conformation possibly for effective supramolecular interaction through H-bonding. The amine derivatization keeps thioether and carboxylic group to lie on either side of the 1,2,4-triazole plane as pendent arms away from the coordination sphere due to favourable and dominant bridging mode by triazole. These dangling arms are only involved in supramolecular interactions. The torsion angle C10–C11–S12A–C13A is 54.8° which is completely different from that of β-DL methionine which is 174.9° [32] and all the carbon atoms and sulfur atoms form an almost-planar zigzag chain. But the torsion angle C7–C6–C10–C11 of 173.3° indicates that main chain carbon atoms lie in a plane away from thiomethyl group.

What makes this polynuclear complex distinctive is due to the dual contribution from its ligand. Here **L4** not only acts as a bridging ligand but also as anion due the presence of deprotonable carboxylic group. Such ionised carboxylate group was reported for a Pt(II) complex where coordination from N and thiomethyl sulfur is observed thus creating a new sterogenic centre at the sulfur atom [33]. The chelating coordination possibility of the amino and carboxylate functions (N, O) is common in underivatized methionine or in its Schiff base form [7f], which is skipped in **6**. A recent report indicates the use of soft-hard recognition principle in methionine to construct a 3D homochiral coordination network [34]. Choice of O/N/S donor preference for coordination from methionine largely depends on this hard-soft concept over steric encumbrance. In **6** the charge on each metal ion is balanced by the deprotonation of carboxylic group which are engaged in H-bonding. The bond length (C7–O9, 1.223(8) Å; C7–O8, 1.213(8) Å) indicates the resonance stabilized double bond after deprotonation. The ethyl(methyl)sulfane group ($-CH_2-CH_2-S-CH_3$) was found to be twofold disordered. The two $S-CH_3$ groups are positioned on opposite sides of the ethyl group. Site occupancy factors were fixed at 65/35%. All coordinated water molecules are involved in H-bonding, with oxygen atom of carboxylate group belonging to different molecules [35]. The plane containing chiral centre carrying carboxylic moiety tilts ~32° away from orthogonality with respect to triazole plane, favouring two strong hydrogen bonding (O8···H14A, 1.85 Å; O9···H14B, 2.01 Å). Thus carboxylic group on each ligand and aqua ligands on terminal zinc act as chain binders establishing the supramolecular interaction (at the periphery) and form a 3D chain. Thus a dense H-bonding network can be seen in this structure (Table 3, Fig. 3). Recent reports highlight the importance of H-bonding of zinc bound water molecules on catalytic activity [36]. It was observed that functional mimics of metallo-β-lactamases catalytically hydrolyze β-lactam substrates, such as oxacillin and penicillin G. The high β-lactamase activity of such compounds was ascribed to the presence of zinc bound water molecules that is activated by being H-bonded to acetate substituent [36].

5.3. β-Lactamases assay

The production of β-lactamases is the most common mechanism of bacterial resistance to β-lactam antibiotics, i.e. penicillins, cephalosporins, and carbapenems [37]. These defence enzymes pose serious medical problems, mainly in hospitals because they rapidly hydrolyze drugs. Most of β-lactamases are serine-proteases (classes A, C and D) against which selective β-lactam inhibitors,

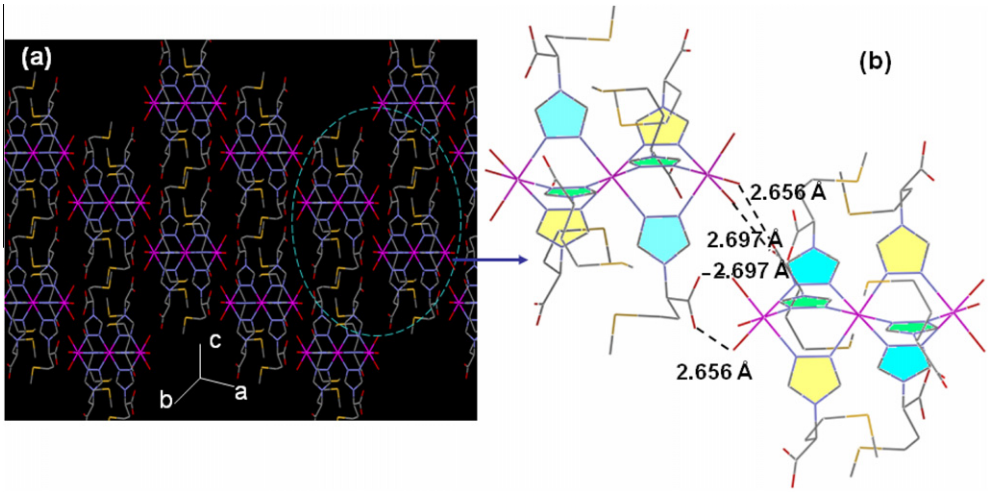

Fig. 3. (a) Crystal packing showing supramolecular aggregation of trinuclear motif in **6**. (b) Expanded view showing role of H-bonding in expanding dimensionality.

Table 4
β-Lactamase inhibitory activity test. Results given as percentages (%) of the initial activity (±5%).

Molecule	BcII (B1)	CphA (B2)	L1 (B3)
L1	100	93	100
L2	100	92	99
L3	91	91	93
L4	79	88	100
L5	91	77	99

such as tazobactam, have been developed and marketed for co-administration with antibiotics [38]. Metallo-β-lactamases (i.e. zinc proteases) constitute the class B [37]; presently, none of the inhibitors of zinc-β-lactamases has emerged for therapeutical use. The search for non-β-lactam compounds, susceptible to form Zn^{II} complexes, could be a valuable strategy to discover inhibitors of class B β-lactamases [39]. Accordingly, the **L1**-**L5** ligands were evaluated for their capacity to inactivate *BcII*, *CephA*, and *L1* enzymes. These are metallo-β-lactamases of sub-classes B1, B2 and B3, respectively. *CephA* exists mainly in the mono-zinc form, while *L1* forms a dinuclear active site [40]; the question of one or two Zn^{II} ions in the class of *BcII* is still open [41].

The tested compounds were pre-incubated with the enzymes (30 min 30 °C) before addition of imipenem antibiotic. The enzymatic residual activity was determined by monitoring the drug hydrolysis at 300 nm. The results of Table 4 are expressed in percentages (%) of the initial activity: it means that low% values indicate active inhibitors. In this assay, the limit for considering a tested compound as potential 'hit' is fixed at 80%. Clearly our ligands are very weak inhibitors of class B β-lactamases. However, one compound (**L4**) can be retained as a modest inhibitor of *BcII* enzyme. As a matter of fact, the **L4** ligand is able to form a polynuclear Zn^{II} complex, as shown by the X-ray diffraction data. The *BcII* inhibition may result from the complexation of one or two zinc ions of the active site by 4-(methylthio)-2-(4H-1,2,4-triazole-4-yl)butanoic acid molecules.

6. Conclusion

The versatility of transamination on amino acid derivatives was illustrated with the synthesis of novel scaffolds (**L1**-**L5**) whose 1,2,4-triazole moiety is linked with either carboxylic acid (ester), phosphonic ester or methyl mercaptan group. Our on-going investigations prove that 1,2,4-triazole functionalized amino acids/esters are useful synthons in the design of multi-functional materials. Different $Zn(L)_2$-type neutral complexes have been formed in solution and identified by routine spectroscopies and elemental analysis. The capacity of **L1**–**L5** to complex Zn^{II} ions has been exploited for the inhibition of metallo-β-lactamases: the activity recorded for **L4** (i.e. the triazole derivative of methionine) against *BcII* enzyme may stimulate further developments in medicinal chemistry. Interestingly the solid state structure of the **L4**-zinc complex (complex **6**) could be obtained: complex **6** is the first crystal structure of a triazole derivatised methionine complex, and also represents the first example of a neutral zinc trinuclear complex with three *N*1, *N*2-1,2,4-triazole bridges and no non coordinated anion. It provides promising perspectives for computational studies in spin crossover research [42] as it gives a model of a trinuclear diamagnetic complex without counter-anion while keeping the same size as high-spin iron(II) ions.

Acknowledgments

This work was partly funded by the Fonds National de la Recherche Scientifique-FNRS (FRFC 2.4508.08), the Interuniversity attraction poles IAP-VI (P6/17) INANOMAT and IAP-VI (P6/19) PROFUSA and a Concerted Research Action of the "Communauté Française de Belgique" allotted by the Académie Universitaire Louvain. J. Marchand-Brynaert is a senior research associate of the F.R.S.-FNRS (Belgium).

Appendix A. Supplementary material

CCDC 789414 contains the supplementary crystallographic data for **6**. These data can be obtained free of charge from The Cambridge Crystallographic Data Centre via www.ccdc.cam.ac.uk/data_request/cif. Supplementary data associated with this article can be found, in the online version, at doi:10.1016/j.ica.2010.12.017.

References

[1] E. Boldyreva, Crystalline Amino Acids, a Link between Chemistry, Materials Science and Biology, Springer, Netherlands, 2008. p. 167.
[2] S. Pizzarello, A.L. Weber, Science 303 (2004) 1151.
[3] S.J. Zuend, M.P. Coughlin, M.P. Lalonde, E.N. Jacobsen, Nature 461 (2009) 968.
[4] J.N. Rebilly, J. Bacsa, M.J. Rosseinsky, Chem. Asian J. 4 (2009) 892.
[5] L.F. Ma, X.K. Huo, L.Y. Wang, J.G. Wang, Y.T. Fan, J. Solid State Chem. 180 (2007) 1648.
[6] M.J. Ingleson, J. Bacsa, M.J. Rosseinsky, Chem. Comm. (2007) 3036.

[7] (a) J-J. Zhang, T-L. Sheng, S-M. Hu, S-Q. Xia, G. Leibeling, F. Meyer, Z-Y. Fu, L. Chen, R-B. Fu, X-T. Wu, Chem. Eur. J. 10 (2004) 3963;
(b) J.D. Ranford, J.J. Vittal, D. Wu, X. Yang, Angew. Chem., Int. Ed. 23 (1999) 3498;
(c) E.V. Anokhina, A.J. Jacobson, J. Am. Chem. Soc. 126 (2004) 3044;
(d) A.D. Cutland-Van Noord, J.W. Kampf, V.L. Pecoraro, Angew. Chem., Int. Ed. 41 (2002) 4668;
(e) Md.A. Alam, M. Netaji, M. Ray, Angew. Chem., Int. Ed. 42 (2003) 1940;
(f) A.K. Patra, S. Dhar, M. Netaji, A.R. Chakravarty, Chem. Commun. (2003) 1562;
(g) A. Tovar-Tovar, L. R-Ramirez, A. Campero, A. Romerosa, R. M-Esparza, M.J. Rosales-Hoz, J. Inorg. Biochem. 98 (2004) 1045;
(h) S-J. Chiou, J. Innocent, C.G. Riordan, K-C. Lam, L. Liable-Sands, A.L. Rheingold, Inorg. Chem. 39 (2000) 4347;
(i) U. Brand, M. Rombach, J. Seebacher, H. Vahrenkamp, Inorg. Chem. 40 (2001) 6151;
(j) P.K. Sasmal, A.K. Patra, M. Netaji, A.R. Chakravarty, Inorg. Chem. 46 (2007) 11112.
[8] (a) A. Mantion, L. Massuger, P. Rabu, C. Palivan, L.B. McCusker, A. Taubert, J. Am. Chem. Soc. 130 (2008) 2517;
(b) B. Wisser, A.-C. Chamayou, R Miller, W. Scherer, C. Janiak, Cryst. Eng. Commun. 10 (2008) 461;
(c) B. Wisser, Y. Lu, C. Janiak, Z. Anorg. Allg. Chem. 633 (2007) 1189;
(d) L.F. Ma, L.Y. Wang, J.G. Wang, Y.F. Wang, X. Feng, Z. Anorg. Allg. Chem. 632 (2006) 487.
[9] A.D. Naik, J. Marchand-Brynaert, Y. Garcia, Synthesis 1 (2008) 149.
[10] M.M. Dîrtu, A.D. Naik, J. Marchand-Brynaert, Y. Garcia, J. Phys.: Conf. Ser. 217 (2010) 012085.
[11] A.D. Naik, M.M. Dîrtu, A. Leonard, B. Tinant, J. Marchand-Brynaert, B.-L. Su, Y. Garcia, Cryst. Growth Des. 10 (2010) 1798.
[12] A. Badarou, M.I. Page, Biochemistry 45 (2006) 10654.
[13] M. Hernandez-Valladares, A. Felici, G. Waber, H.W. Adolph, M. Zepperzauer, G.M. Rossolini, G. Amicosante, J.M. Frere, M. Galleni, Biochemistry 36 (1997) 11534.
[14] J.H. Ullah, T.R. Walsh, I.A. Talor, D.C. Emery, C.S. Verma, S. Gamblin, J. Spencer, J. Mol. Biol. 284 (1998) 125.
[15] R.K. Bartlett, I.R. Humphrey, J. Chem. Soc. C (1967) 664.
[16] B. Fohlisch, R. Braun, K.W. Schultze, Angew. Chem., Int. Ed. 6 (1967) 361.
[17] M. Ferrari, G. Jommi, G. Miglierini, R. Pagliarin, M. Sisti, Synth. Commun. 22 (1992) 107.
[18] D. Seyferth, R.M. Marmor, P.H. Hilbert, J. Org. Chem. 36 (1971) 1379.
[19] G.M. Sheldrick, SHELXS-97 and SHELXL-97, Program for Crystal Structure Refinement, University of Göttingen, Germany, 1997.
[20] Y. Garcia, O. Kahn, L. Rabardel, B. Chansou, J.–P. Tuchagues, Inorg. Chem. 38 (1999) 4663.
[21] Y. Boland, P. Herstens, J. Marchand-Brynaert, Y. Garcia, Synthesis 9 (2006) 1504.
[22] T.M. Potewar, S.A. Siddiqui, R.J. Lahoti, K.V. Srinivasan, Tetrahedron Lett. 48 (2007) 1721.
[23] H.O. Bayer, R.S. Cook, W.C. von Meyer, US Patent 382137628, 1974; Chem. Abstr. 76 (1972) 113224.
[24] D. Kantoci, J.K. Denike, W.J. Wechter, Synth. Commun. 26 (1996) 2037.
[25] J. Beck, S. Gharbi, A. Herteg-Fernea, L. Vercheval, C. Bebrone, P. Lassaux, A. Zervosen, J. Marchand-Brynaert, Eur. J. Org. Chem. (2009) 85.
[26] J. Beck, E. Sauvage, P. Charlier, J. Marchand-Brynaert, Bioorg. Med. Chem. Lett. 18 (2008) 3764.
[27] J. Beck, L. Vercheval, C. Bebrone, A. Herteg-Fernea, P. Lassaux, J. Marchand-Brynaert, Bioorg. Med. Chem. Lett. 19 (2009) 3593.
[28] K.A. Siddiqui, M. Bolte, G.K. Mehrotra, Inorg. Chim. Acta 363 (2010) 457.
[29] J.G. Haasnoot, Coord. Chem. Rev. 200 (2000) 131.
[30] U. Heinza, H.-W. Adolph, Cell. Mol. Life Sci. 61 (2004) 2827.
[31] A.L. Spek, G. Vos, Acta Crystallogr., Sect. C39 (1983) 990.
[32] (a) M. Alagar, R.V. Krishnakumar, A. Mostad, S. Natarajan, Acta Crystallogr., Sect. E61 (2005) o1165;
(b) S. Natarajan, N.R. Devi, S.D.M.B. Dhas, S. Athimoolam, Sci. Technol. Adv. Mater. Sci. 9 (2008) 025012.
[33] C. Rothenburger, M. Galanski, V.B. Arion, H. Gorls, W. Weigand, B.K. Keppler, Eur. J. Inorg. Chem. (2006) 3746.
[34] T.T. Luo, L.-Y. Hsu, C.-C. Su, C.-H. Ueng, T.-C. Tsai, K.-L. Lu, Inorg. Chem. 46 (2007) 1532.
[35] R. Taylor, O. Kennard, W. Versichel, J. Am. Chem. Soc. 106 (1984) 244.
[36] (a) A. Tamilselvi, G. Mugesh, J. Biol. Inorg. Chem. 13 (2008) 1039;
(b) A. Tamilselvi, M. Nethaji, G. Mugesh, Chem. Eur. J. 12 (2006) 7797.
[37] P. Macheboeuf, C. Contreras-Martel, V. Job, O. Dideberg, A. Dessen, FEMS Microbiol. Rev. 30 (2006) 673.
[38] A. Bryskier, C. Couturier, J. Lowther, Antimicrob. Agents Chemoter. (2005) 410.
[39] J. Beck, L. Maton, J.L. Habib Jiwan, J. Marchand-Brynaert, Amino acids, 2010, doi: 10.1007/s00726-010-0697-x.
[40] C. Bebrone, Biochem. Pharm. 74 (2007) 1686.
[41] L.I. Llarrull, M.F. Tioni, J. Kowalski, B. Bennett, A.J. Vila, J. Biol. Chem. 282 (2007) 30586.
[42] J.A. Wolny, S. Rackiwtz, K. Achterhold, Y. Garcia, K. Muffler, A.D. Naik, V. Schunemann, Phys. Chem. Chem. Phys. 12 (2010) 14782.